2019

Nonlinear dynamics and control in a tumor-immune system

BOSTON UNIVERSITY

COLLEGE OF ENGINEERING

Thesis

NONLINEAR DYNAMICS AND CONTROL IN A TUMOR-IMMUNE SYSTEM

by

YU XUAN

B.Eng., Beihang University (BUAA), 2016

Submitted in partial fulfillment of the

requirements for the degree of

Master of Science

2019

Approved by

First Reader

Hua Wang, Ph.D.
Associate Professor of Mechanical Engineering
Associate Professor of Systems Engineering

Second Reader

Rebecca Khurshid, Ph.D.
Assistant Professor of Mechanical Engineering
Assistant Professor of Systems Engineering

Third Reader

John Baillieul, Ph.D.
Distinguished Professor of Mechanical Engineering
Distinguished Professor of Systems Engineering
Distinguished Professor of Electrical and Computer Engineering

ACKNOWLEDGMENTS

I would like to express my special thanks of gratitude to my advisor, Dr. Hua Wang for his guidance and support. The results presented in this thesis would not have been possible without his patience, motivation and immense knowledge.

I am very grateful to Dr. John Baillieul, Dr. Rebecca Khurshid and Dr. Sean Andersson for serving on my thesis committee and for the interests they have expressed in my research.

I would like to thank Ms. Anna Masland who is the master's program administrator in my department. She has assisted me a lot in scheduling the thesis process. I would also like to thank Mt. Brendan McDermott, the thesis/dissertation coordinator from Mugar Memorial Library at Boston University, for his assistance in formatting the thesis.

To my parents and friends, I would express my most profound appreciation for their love and continuous encouragement.

NONLINEAR DYNAMICS AND CONTROL IN A TUMOR-IMMUNE SYSTEM

YU XUAN

ABSTRACT

Advances in modeling tumor-immune dynamics and therapies offer deeper understandings of the mechanism of tumor evolution in the interdisciplinary field of mathematics and immune-oncology. The main mathematical models are constructed in terms of ordinary differential equations (ODEs) or partial differential equations (PDEs) and analyzed through tools such as Poincaré map, simulation, or numerical bifurcation analysis to understand the system properties. These models succeed in characterizing essential features of tumor behaviors including periodic bursts and the existence of latency. In relationship to practice, these models are also applied to estimate the feasibility and efficacy of treatments ranging from traditional chemotherapy to immunotherapy (ACI).

In recent literature, there have been applications of control methods such as optimal control, hybrid automata, and feedback linearization-based tracking control with almost disturbance decoupling in the studies of tumor-immune systems. This thesis presents an attempt to apply the bifurcation control method with washout filters in tumor treatments.

This thesis research investigates the dynamics and controlling of the tumor-immune response of immunotherapies, mainly the Adoptive Cell Immunotherapy (ACI) and Interleukin-2 (IL-2). The first part of the thesis presents the nonlinear dynamics of the classic nonlinear ODE tumor-immune model given by Denise Kirschner and John

Carl Panetta in 1998. This model concentrates on the nonlinear phenomena of the tumor-immune system under immunotherapies, primarily the bifurcation phenomenon along with the antigenicity of effector cells. Bifurcation phenomena refer to the qualitative changes in system dynamics due to quasi-static changes in system parameters. Antigenicity refers to a capability to distinguish tumor cells from healthy cells. The Kirschner-Panetta model captures a saddle-node bifurcation and a Hopf bifurcation of the tumor-immune response, which separates the tumor evolution into three stages, the "dangerous equilibrium", the periodic recurrence, and the "safe equilibrium".

The second part applies and analyzes several control strategies on the immunotherapies based on the KP model in order to eradicate tumors or inhibit tumor growths. The first section studies the combination immunotherapy of ACI and IL-2 as an open-loop control system based on Kirschner's work, which generates a locally asymptotically stable equilibrium. In the second section, this thesis provides a new idea of treatment in the tumor-immune system, that is a closed-loop control strategy taking advantage of its bifurcation structure by applying dynamic feedback control with a washout filter of ACI or IL-2. Bifurcation control moves the Hopf bifurcation point without changing the equilibrium structure as the bifurcation parameter varies. In this tumor-immune case, the linear dynamic feedback control with a washout filter of ACI could either extend the "safe equilibrium" region or reduce the amplitude of the tumor population at the stage of tumor recurrence. In addition, other bifurcation amplitude controls of either ACI or IL-2 are attempted to reduce the amplitudes of periodic orbits of the tumor immune system but without obvious effects.

TABLE OF CONTENTS

LIST OF TABLES

LIST OF FIGURES

LIST OF ABBREVIATIONS

ACI	Adoptive cellular immunotherapy
IL-2	Interleukin-2
KP model	the Kirschner and Panetta model
ODE	Ordinary differential equation
PDE	Partial differential equation
ROA	Region of attraction

CHAPTER ONE INTRODUCTION

Cancer is one of the leading fatal diseases. Though surgical resection, chemotherapy, and radiotherapy have played a significant role in tumor or cancer treatment in clinical, there is an urgent need for more effective therapies against neoplasms. As a result, immunotherapy has greatly progressed in recent decades. In the 1970s, there was considerable enthusiasm for immunotherapeutic approaches that apply nonspecific substances to stimulate immune systems against tumor growth, but those approaches were abandoned soon [25]. Since the 1980s, an alternate method, the so-called passive or adoptive immunotherapy, has made considerable headways [2]-[12]. The passive immunotherapy refers to a systematic transfer of the substances or cells that already own anti-tumor abilities. In this thesis, immunotherapy refers in particular to passive immunotherapy.

The immunotherapy usually includes cytokines and adoptive cellular immunotherapies (ACI). According to [15], “Cytokines are protein hormones that mediate both natural and specific immunity. They are produced mainly by activated T cells (lymphocytes) during cellular-mediated immunity. Interleukin-2 (IL-2) is the main cytokine responsible for lymphocyte activation, growth, and differentiation.” ACI is an immunological treatment that implants into tumor-bearing hosts the immune cells (effector cells) whose anti-tumor features have been activated in vitro. Lymphokine-activated killer cell (LAK) therapy and tumor infiltrating lymphocyte (TIL) therapy are two principal approaches to achieve ACI.

In the interdisciplinary field of mathematics and immunology, advances in

modeling tumor-immune dynamics and therapies offer a deeper understanding of the mechanism of tumor evolution. The main mathematical models are constructed in terms of ordinary differential equations (ODEs) or partial differential equations (PDEs) [1] and analyzed through tools such as Poincaré map, simulation, or numerical bifurcation analysis to understand the system properties. ODE models describe the temporal dynamics of tumor-immune interaction at the cellular or molecular level, and PDE models involve more factors such as spatial effects. These models succeed in characterizing essential features of tumor behaviors, such as periodic bursts and the existence of latency. In relationship to practice, these models are also applied to estimate the feasibility and efficacy of treatments ranging from traditional chemotherapy and radiotherapy to immunotherapy (ACI). This thesis focuses on a specific ODE model.

Potentially lethal tumor cells might keep in a "safe" state that the population persists to be harmlessly small for a host over a long period; but the small population might boom all of a sudden in the lack of immunological surveillance. Kuznetsov etc. [14] relate these special phenomena of "dormant state" and "sneaking through" with nonlinear dynamics via an ODE model. This model quantitatively describes the interaction between two central populations, the effector cells, and tumor cells. This model was shown to possess stable spirals, but its dynamics is not rich enough since the Dulac-Bendixson criterion proves that there does not exist stable closed orbits.

Kirschner and Panetta [15] furthered Kuznetsov's model by incorporating other mathematical modellings of tumor-immune interactions [16][17][18][19]. This thesis is based on the Kirschner and Panetta model (KP model). They constructed a three-

dimensional ODE model of tumor-immune interactions under immunotherapy. Comparing to Kuznetsov's model that focuses on the anti-tumor mechanism of immune systems, the KP model tends to guide oncotherapy, especially the immunotherapy, by introducing treatment terms of adoptive cellular immunotherapy (ACI) and Interleukin-2 (IL-2). The KP model captures a periodic response of tumor-immune which corresponds to the neoplasm recurrence in clinical. They also indicate that a combination treatment of ACI and IL-2 works better than single treatments with either ACI or IL-2. Only the combination treatment could eliminate tumor cells.

The classic KP model is simple enough to motivate further research work of modeling tumor-immune systems and applications of mathematical control [20]. Phillis etc. [21] develop a mixed-treatment model combining immunotherapy and chemotherapy, based on which Rihan etc. [22] have also studied an optimal control problem with delay in the effect of effector cells. Mallet etc. [23] construct a hybrid cellular automaton based on the temporary results from the KP model. Chien etc. [24] apply feedback linearization with almost disturbance decoupling control directly to the KP model, and the method assumes that all state variables are measurable using a programmable research micro-pump and computer, such as the Cellometer Auto T4 Cell Counter.

In recent years, there has also been a growing body of research on control of nonlinear dynamical systems exhibiting bifurcation phenomena. The objective of the bifurcation control is to modify the system behaviors by relocating bifurcation points or changing the stability properties of bifurcation branches. Bifurcation control has been

applied to a wide range of applications such as voltage collapse in power systems, rotating stall and surge in compression systems, cardiac dynamics with arrhythmias, to name a few [26]. Based on a transformed Lorenz equation, the work in [27] shows dynamic bifurcation control with washout filters can change the location and stabilize Hopf bifurcations without changing the equilibrium structure of the system.

This thesis research investigates the dynamics and controlling of the tumor-immune response of immunotherapies, mainly the ACI and the IL-2. The first part of the thesis presents the nonlinear dynamics of the classic nonlinear ODE tumor-immune model given by Denise Kirschner and John Carl Panetta in 1998. This model concentrates on the nonlinear phenomena of the tumor-immune system under immunotherapies, primarily the bifurcation phenomenon along with the antigenicity of effector cells. Bifurcation phenomena refer to the qualitative changes in system dynamics due to quasi-static changes in system parameters. Antigenicity refers to a capability to distinguish tumor cells from healthy cells. The KP model captures a saddle-node bifurcation and a Hopf bifurcation of the tumor-immune response, which separates the tumor evolution into three stages, the “dangerous equilibrium”, the periodic recurrence, and the “safe equilibrium”.

The second part applies and analyzes several control strategies on the immunotherapies based on the KP model in order to eradicate tumors or inhibit tumor growths. The first section studies the combination immunotherapy of ACI and IL-2 as an open-loop control system based on Kirschner’s work, which generates a locally asymptotically stable equilibrium. In the second section, this thesis provides a new idea

of treatment in the tumor-immune system, that is a closed-loop control strategy taking advantage of its bifurcation structure by applying dynamic feedback control with a washout filter of ACI or IL-2. Bifurcation control moves the Hopf bifurcation point without changing the equilibrium structure as the bifurcation parameter varies. In this tumor-immune case, the linear dynamic feedback control with a washout filter of ACI could either extend the “safe equilibrium” region or reduce the amplitude of the tumor population at the stage of tumor recurrence. Furthermore, other bifurcation amplitude controls of either ACI or IL-2 are attempted to reduce the amplitudes of periodic orbits of the tumor immune system but without obvious effects.

CHAPTER TWO NONLINEAR ANALYSIS OF THE TUMOR-IMMUNE INTERACTIONS

2.1 Preliminaries of Bifurcation Theory

Phenomena of nonlinear systems can be rich and complex, and the phenomena might become more intricate when parameters change in corresponding systems. To systematically understand the nonlinear dynamics along with varying parameters, we can classify the complex nonlinear dynamics into distinct patterns according to the existence and stability properties of equilibrium points, period orbits or other invariant subsets. *Bifurcation* refers to the critical situation that those essential properties of a nonlinear system undergo qualitative transformations with quasi-static changes of system parameters. These system parameters are defined as *bifurcation parameters*, and the parameter values at which critical changes occur are called *bifurcation points* [13]. *Bifurcation diagram* is a graphically descriptive tool for bifurcation analysis which structurally depicts the relationship between the essential nonlinear properties and bifurcation parameters.

Consider a one-parameter finite dimensional system

$$\dot{\boldsymbol{x}} = \boldsymbol{f}(\boldsymbol{x}, c), \tag{2.1}$$

where $\boldsymbol{x} \in \mathbb{R}^n$ is the state vector, $c \in \mathbb{R}$ is the bifurcation parameter, and $\boldsymbol{f}$: $\mathbb{R}^{n+1} \to \mathbb{R}^n$ is the smooth vector field. Without losing any generality, consider the situation that the origin $\boldsymbol{x} = \boldsymbol{0}$ is an equilibrium point and the Jacobian matrix $J \triangleq \frac{\partial \boldsymbol{f}}{\partial \boldsymbol{x}}\Big|_{\boldsymbol{x}=\boldsymbol{0}, c=0}$ owns eigenvalues with zero real parts. Suppose that the origin loses stability, i.e., any the

Jacobian eigenvalue crosses the complex axis, when c changes sign, then a bifurcation point occurs at $c = 0$.

Figure 2.1 summaries the nondegenerate bifurcations. *Saddle-node bifurcation* (a) results from a collision between a stable node equilibrium point and a saddle equilibrium point. As the bifurcation parameter pass through the bifurcation point, both stable equilibrium branch and unstable equilibrium branch generate together. *Transcritical bifurcation* (b) refers to the crossing point of two equilibrium branches. The equilibrium branches change their stability properties after an intersection. *Pitchfork bifurcation* (c and d) combines generations of new branches and changes of stability. Single equilibrium branch changes its stability property when traversing the bifurcation point, as well as two equilibrium branches that remain the original stability arise above and below. These bifurcations are collectively called *stationary bifurcation* where only equilibrium points take place. *Hopf bifurcation* (e and f) looks similar to Pitchfork bifurcation. The difference is that two branches of limit cycle arise here instead of two equilibrium branches in the pitchfork bifurcation. Besides, *supercritical bifurcation* (c and e) and *subcritical bifurcation* (d and f) classify the bifurcation phenomena into safe and dangerous cases. The dynamics of supercritical case transfer smoothly, while those of subcritical case, transcritical and saddle-node always result in a system hysteresis or state jumps due to the disappearance of stable branches [13].

In this thesis research, both saddle-node bifurcation and Hopf bifurcation are discovered and discussed. Therefore, it is necessary to present the mathematical description of both stationary bifurcation and Hopf bifurcation.

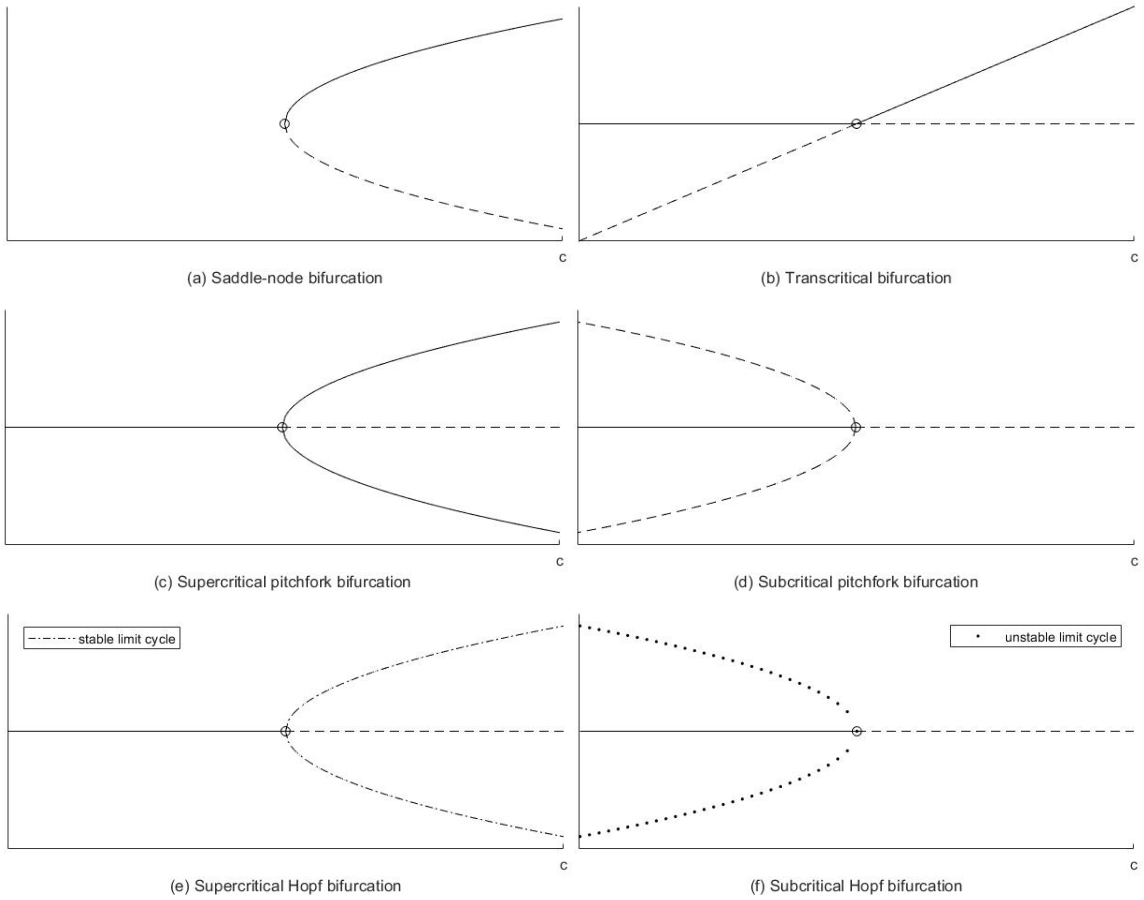

Figure 2.1 Nondegenerate bifurcation diagrams (solid line: stable equilibrium, dash line: unstable equilibrium, circle: bifurcation points).

2.1.1 Stationary Bifurcation

Transform the system, equation (2.1), into a linearized form

$$\dot{\boldsymbol{x}} = \mathrm{A}(c)\boldsymbol{x} + \boldsymbol{f}(\boldsymbol{x};\ \boldsymbol{c}) \qquad (2.2)$$

where $\boldsymbol{f} \in C^k(\mathbb{R}^n)$ with k ≥ 3, $\boldsymbol{f}(\boldsymbol{x_0};\ \boldsymbol{c}) = \boldsymbol{0}$, $\frac{\partial \boldsymbol{f}}{\partial \boldsymbol{x}}(\boldsymbol{x_0};\ \boldsymbol{c}) = \boldsymbol{0}$ for all sufficiently small $|c - c_0|$, and c_0 is the value of c at the bifurcation point.

A stationary bifurcation is guaranteed to occur when a single real eigenvalue goes from being negative to being positive as c passes through the value c_0. More precisely,

the origin of the system (2.1) undergoes a stationary bifurcation at the critical parameter value $c = 0$ if the following hypothesis hold [35][36]:

1. Vector field $\boldsymbol{f}$ in the system (2.1) is sufficiently smooth in $\boldsymbol{x}$, c, and $\boldsymbol{f}(\boldsymbol{x_0};\ \boldsymbol{c}) = \boldsymbol{0}$ for all c in a neighborhood of 0. The Jacobian $\mathrm{A}(c) \triangleq \frac{\partial \boldsymbol{f}}{\partial \boldsymbol{x}}(\boldsymbol{0}, \boldsymbol{c})$ possesses a simple real eigenvalue $\lambda(c)$ such that $\lambda(0) = 0$ and $\lambda'(0) \neq 0$;
2. All eigenvalues of the critical Jacobian $\mathrm{A}(c)$ besides 0 have negative real parts.

2.1.2 Hopf Bifurcation

Assume that the linear part $\mathrm{A}(c)$ in equation (2.2) at the origin has a pair of eigenvalues $\lambda_{1,2}(c) = \alpha(c) \pm \mathrm{i}\omega(c)$ with $\alpha(c_0) = 0$ and $\omega(c_0) \neq 0$. Furthermore, suppose that the pair of eigenvalues cross the imaginary axis with nonzero speed, i.e.,

$$\frac{\partial \alpha}{\partial c}(c_0) \neq 0, \tag{2.3}$$

which is known as the *transversality* condition for the crossing of the eigenloci at the imaginary axis. Then in any neighborhood U of the point x_0 and for any given $\varepsilon > 0$, there is a $|\bar{c} - c_0| < \varepsilon$ such that the differential equation (2.2) has a nontrivial periodic orbit in U. In this case, the system is said to undergo a *Hopf bifurcation* at the bifurcation point $(\boldsymbol{x}_0, c_0)$ [35][36].

2.2 Kirschner and Panetta's Tumor-Immune Model

This thesis research studies the dynamics and control of tumor-immune system under immunotherapy based on the KP model. Here is the state model:

$$\frac{dx_1}{dt} = cx_2 - \mu_2 x_1 + \frac{p_1 x_1 x_3}{g_1 + x_3} + u_1 \tag{2.4}$$

$$\frac{dx_2}{dt} = r_2 x_2(1 - bx_2) - \frac{a x_1 x_2}{g_2 + x_2} \tag{2.5}$$

$$\frac{dx_3}{dt} = \frac{p_2 x_1 x_2}{g_3 + x_2} - \mu_3 x_3 + u_2 \tag{2.6}$$

with the initial condition:

$$\boldsymbol{x}(0) = [x_{10}, x_{20}, x_{30}]^T \tag{2.7}$$

and the output equation:

$$y = x_2. \tag{2.8}$$

Here the state variable x_1, x_2, x_3 represents the population of effector cells, the population of tumor cells, and the concentration of IL-2, respectively; u_1, u_2 refers to two kinds of immunotherapy, ACI and IL-2.

It is significant to understand the nonlinear terms contained in the KP model as it explains the mechanism of tumor-immune response through nonlinear phenomena. The KP model mainly contains two nonlinear terms, the logistic growth rate, and the Michaelis-Menten kinetics.

The logistic function is in the form of

$$l(v) = \alpha(1 - \beta v), \tag{2.9}$$

where α, β are constants. In the dynamic equation

$$\frac{dv}{dt} = l(v)v, \tag{2.10}$$

the logistic function serves as the growth rate. Figure 2.2 shows the solution of equation (2.10). For v close to zero, $l(v)$ approximates to α, then v grows exponentially following

$e^{\alpha t}$; as v increases, $l(v)$ approaches to 0, then asymptotically v grows to $1/\beta$. In biological dynamics, $1/\beta$ refers to the carrying capacity of a substance v [1].

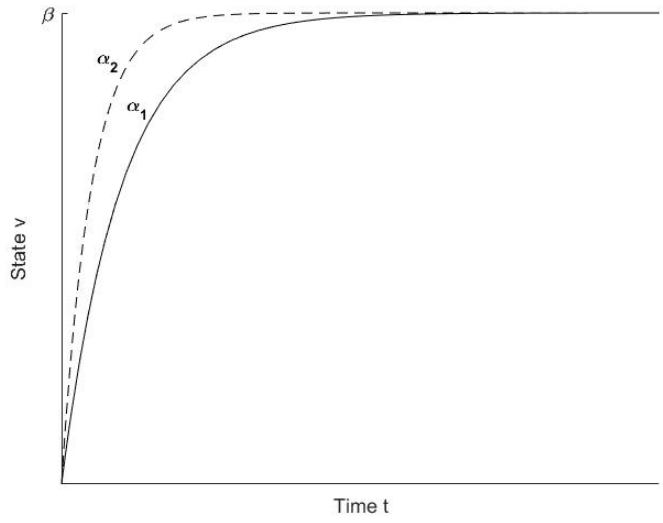

Figure 2.2 Logistic function ($\alpha_1 < \alpha_2$)

Michaelis-Menten kinetics, a classic enzyme kinetics, relates the enzyme reaction rate k to the concentration of a substance v as

$$k(v) = \frac{\alpha v}{\beta + v}. \tag{2.11}$$

Here constant α is the upper limit of $k(v)$, and constant β refers to the half-lifespan of $k(v)$, i.e., the value of v when $k(v)$ reaches half value. The Michaelis-Menten Kinetics is shown in Figure 2.3.

This model simplifies and summaries the immune mechanism responding to tumors as an interaction among effector cells, tumor cells, and cytokine IL-2. The appearance of tumor cells activates the effector cells to proliferate and to secrete IL-2. IL-2 would not eliminate tumor cells directly but work as a stimulator for the effector cells. Finally, effector cells could kill the identified tumor cells.

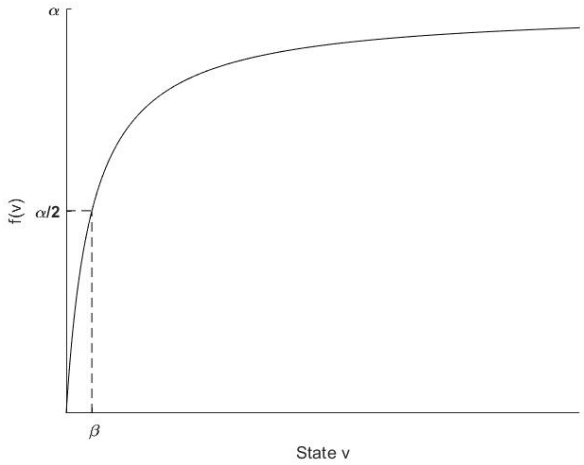

Figure 2.3 Michaelis-Menten Kinetics $k(v)$

It is challenging to account total amounts of biological components in practice. Instead, the model describes the evolution by the average difference in population or concentration within time dt in both proliferation part (positive) and death part (negative). According to [15], the first equation describes the rate of change for the effector-cell population. The defense mechanism of immune systems against tumors is directly activated by the tumor cells (Term1), as well as indirectly stimulated by the IL-2 (Term 3). In Term 1, the growth rate c means the antigenicity of the tumor. *Antigenicity* describes the immunological surveillance capability of effector cells, the ability to distinguish tumor cells from other normal cells, and it ranges from 0 to 0.05 individually. The other growth term (Term 3) models the proliferation of effector cells stimulated by IL-2 that is produced by the effector cell itself in a both autocrine and paracrine manner. The Michaelis-Menten form indicates the saturated effects of the immune response with the highest growth rate of g_1. Term 2 represents the natural death of immune cells with an average lifespan of $1/\mu_2$ days. The final term u_1 refers to the treatment that externally provides effector cells such as LAK or TIL cells.

The second equation marks the change rate in the tumor population with a logistic growth rate

$$r_2(1 - bx_2). \tag{2.12}$$

For the tumor evolution

$$\frac{dx_2}{dt} = r(\cdot)x_2 - \frac{ax_1x_2}{g_2 + x_2}, \tag{2.13}$$

there are three primary growth patterns differentiated by the growth rate $r_2(\cdot)$, the constant, logistic [28] and Gompertz [29][30][31] growth rate. The tumor grows exponentially with a constant r or grows with limits in the latter two forms, where the Gompertz is smoother but much more complicated. Term 2 describes the immune clearance of tumor cells with a limit effect at rate a. (The Michaelis-Menten form could also account for the effects of a solid tumor, i.e., only a portion of the tumor mass comes in contact with the immune system cells.)

Different from previous equations, Equation 3 gives the change rate of IL-2 concentration. The source of IL-2 is the effector cells stimulated by tumors, and these activated effector cells secrete IL-2 with limited speed as modeled in Michaelis-Menten kinetics form. The next term (μ_3) represents the natural loss rate of IL-2. Finally, u_2 is a treatment term that represents an external input of IL-2 into the system.

2.2.1 Parameters and Scaling

Kirschner gives parameters in this state model based on the papers [19][14][25]. Noted that the units of the value given in Table 2.1 are in $days^{-1}$, except for $g_1,\ g_2,\ g_3$ and b whose units are volume.

$\boldsymbol{c}$	$\boldsymbol{a}$	$\boldsymbol{b}$	$\boldsymbol{p_1}$	$\boldsymbol{p_2}$	$\boldsymbol{r_2}$
$[\mathbf{0}, \mathbf{0.05}]$	1	1×10^{-9}	0.1245	5	0.18
$\boldsymbol{g_1}$	g_2	g_3	μ_2	μ_3	
$\mathbf{2 \times 10^7}$	1×10^5	1×10^3	0.03	10	

Table 2.1 parameters in the KP model

This model is stiff for simulation due to the wide range of parameters. Appropriate scaling is necessary to carry out the numerical analysis. Normalizing the population of tumor cells is one option of the non-dimensional scaling. $1/b$ refers to the carrying capacity of the tumor cells. As a result, all the cell number units related values are non-dimensionalized by 1/b. Moreover, the time units related values are non-dimensionalized by r_2 according to Kirschner's recommendation.

Set

$$E_0 = T_0 = I_{L0} = 1/b \tag{2.14}$$

$$t_s = r_2, \tag{2.15}$$

the scaling of each variable and parameter is shown below.

$$\bar{x}_1 = \frac{x_1}{E_0}, \quad \bar{x}_2 = \frac{x_2}{E_0}, \quad \bar{x}_3 = \frac{x_3}{I_{L0}}, \quad \tau = t_s t, \quad \bar{c} = \frac{cT_0}{t_s E_0}, \quad \bar{a} = \frac{aE_0}{t_s T_0},$$

$$\bar{p}_1 = \frac{p_1}{t_s}, \quad \bar{p}_2 = \frac{p_2 E_0}{t_s I_{L0}}, \quad \bar{g}_1 = \frac{g_1}{I_{L0}}, \quad \bar{g}_2 = \frac{g_2}{T_0}, \quad \bar{g}_3 = \frac{g_3}{T_0}, \quad \bar{b} = bT_0,$$

$$\bar{\mu}_2 = \frac{\mu_2}{t_s}, \quad \bar{\mu}_3 = \frac{\mu_3}{t_s}, \quad \bar{r}_2 = \frac{r_2}{t_s}, \quad \bar{u}_1 = \frac{u_1}{t_s E_0}, \quad \bar{u}_2 = \frac{u_2}{t_s T_0}, \quad \bar{u}_3 = \frac{u_3}{t_s I_{L0}}. \tag{2.16}$$

The corresponding state model after Non-dimensional scaling gives the following equations.

$$\frac{d\bar{x}_1}{d\tau} = \bar{c}\bar{x}_2 - \bar{\mu}_2\bar{x}_1 + \frac{\bar{p}_1\bar{x}_1\bar{x}_3}{\bar{g}_1 + \bar{x}_3} + \bar{u}_1 \tag{2.17}$$

$$\frac{d\bar{x}_2}{d\tau} = \bar{r}_2\bar{x}_2\left(1 - \bar{b}\bar{x}_2\right) - \frac{\bar{a}\bar{x}_1\bar{x}_2}{\bar{g}_2 + \bar{x}_2} \tag{2.18}$$

$$\frac{d\bar{x}_3}{d\tau} = \frac{\bar{p}_2\bar{x}_1\bar{x}_2}{\bar{g}_3 + \bar{x}_2} - \bar{\mu}_3\bar{x}_1 + \bar{u}_2 \tag{2.19}$$

In this thesis, all scaled parameters and variables are marked by hats except for scaled time τ.

2.3 Bifurcation and Dynamic Analysis for Non-Treatment Case

This section revises Kirschner's work in the nonlinear dynamics analysis of the tumor-immune system without control (non-treatment case), equation (2.20) – (2.22). Understanding the mathematical dynamics and the corresponding immunological implication of the KP model is a vital prerequisite of the thesis research.

$$\frac{dx_1}{dt} = cx_2 - \mu_2 x_1 + \frac{p_1 x_1 x_3}{g_1 + x_3} \tag{2.20}$$

$$\frac{dx_2}{dt} = r_2 x_2(1 - bx_2) - \frac{ax_1 x_2}{g_2 + x_2} \tag{2.21}$$

$$\frac{dx_3}{dt} = \frac{p_2 x_1 x_2}{g_3 + x_2} - \mu_3 x_3 \tag{2.22}$$

Although the nonlinear system is difficult to solve analytically, numerical methods can be employed to gain an understanding of the dynamics of the tumor-immune system. This research uses AUTO (07p) for the bifurcation analysis along with parameter *c*, the antigenicity, and MATLAB for the temporal dynamical simulation at fixed *c*.

AUTO [32][33][34] is a powerful continuation and bifurcation analysis software for differential equations. Given an initial state near equilibrium branches, AUTO can automatically approach an equilibrium point, and numerically analyze the stability of either equilibriums or limit cycles, then continue the branches point by point.

The combined usage of bifurcation analysis and simulation helps to reveal the non-local dynamics of the model, and it goes as following way. The bifurcation analysis along the antigenicity c predicts the non-local dynamical trends of the states at each fixed c, which also guide the selection of the initial states in simulation. In turn, simulations in Matlab serve as initial conditions for the numerical calculation in AUTO. AUTO is able to do the continuation of solutions of ODEs based on the appropriate initial guess of equilibrium points. Simulations are also supplements for several situations that AUTO is unable to solve, such as chaos, though not found in this research.

2.3.1 Bifurcation Diagram and Simulation Results

Human immune systems have multiple defense mechanisms in the face of external invasions or internal abnormal variations. Different than external invader such as virus, the tumor is one of the internal abnormal variations. Making out those tumor cells is the precondition for a successful self-immune defense. Furthermore, different levels of the identifying capability of immune systems activate different defense mechanisms. In other words, human immune responses vary with the antigenicity of effector cells.

Bifurcation analysis, especially bifurcation diagram, of the KP model shows the diversity of tumor-immune response. To be specific, the nonlinear dynamics of non-treatment model changes qualitatively along with parameter c. As shown in Figure 2.4,

the nonlinear dynamics of the non-dimensional tumor population presents a “foot-like” bifurcation structure along with the antigenicity c between $[-0.01, 0.05]$.

Note that this research studies the non-local dynamics of the system within the nonnegative state space as the negative state is meaningless in neither the natural immune response nor the clinical immunotherapy. For the antigenicity, though the area with negative values, $c \in [-0.01,0)$, is insignificant in practice, it shows the bifurcation structure of the tumor evolution.

There are two bifurcation branches are captured. One branch is a lateral straight line representing an unstable equilibrium point at origin independent of c, which can be easily captured by solving the state model with all zero states. Figure 2.4 shows the other bifurcation branch. The “foot-like” bifurcation branch changes dramatically with c. Consider the nonnegative c part of the bifurcation diagram, two bifurcations points c_0 and c_1 separate the graph into three rectangular areas with distinct nonlinear dynamical patterns. AUTO shows that c_0 is a fold, and c_1 is a Hopf bifurcation. Figure 2.5 zooms in on the surrounding area of c_0. It shows that the exact type of bifurcation point c_0 is not clear. It is either a saddle-node bifurcation or a homoclinic bifurcation depends on whether the saddle point collides with the limit cycle branch or not. Auto shows that the limit cycle branch is approaching to c_0 but not touch it. Further analysis is necessary for the judgment. However, this uncertainty would not affect the understanding of the system dynamics and the following researches.

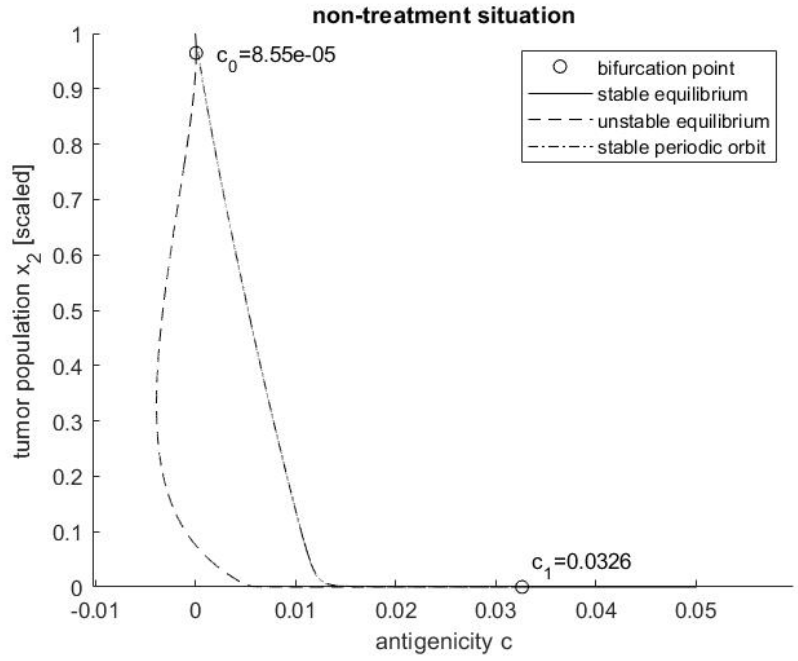

Figure 2.4 Bifurcation diagram of the non-treatment KP model

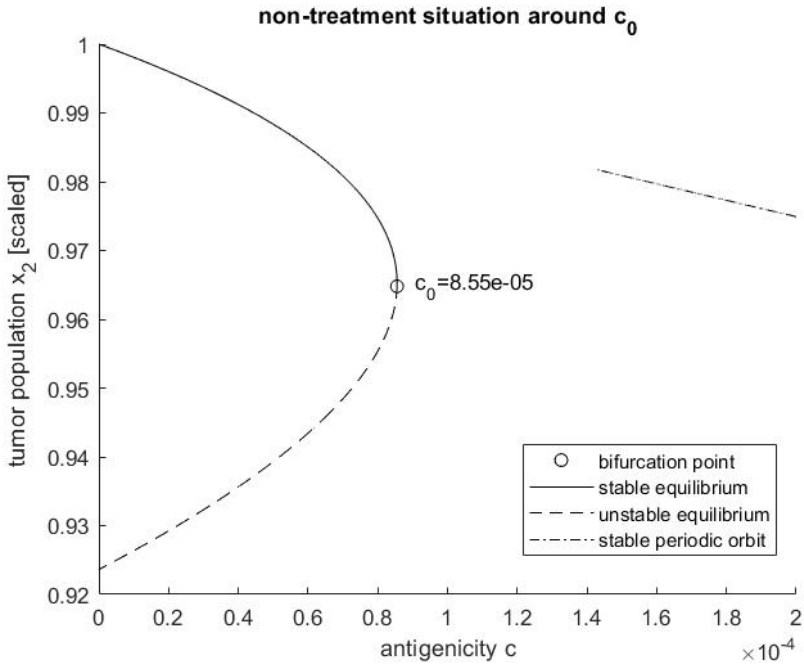

Figure 2.5 Bifurcation diagram of the non-treatment KP model in the neighborhood of c_0

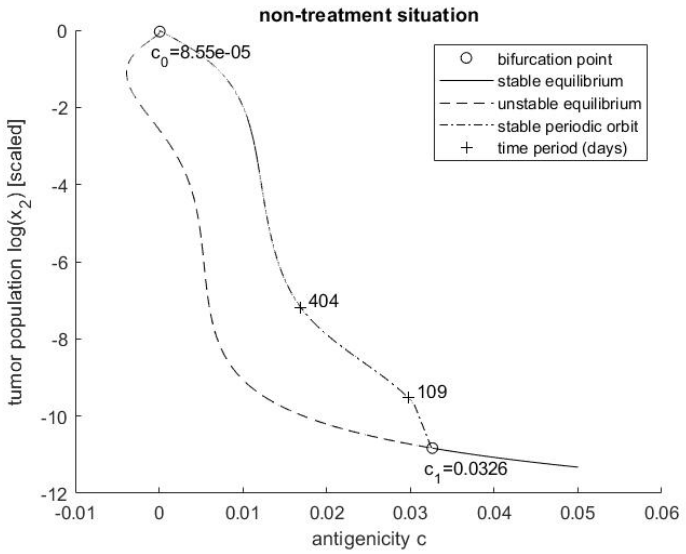

Figure 2.6 Bifurcation diagram of the non-treatment KP model in semi-logarithmic coordinates

Next, the dynamics of the non-treatment KP model within each c area is simulated by Matlab with a uniform initial condition that $\bar{\boldsymbol{x}}(0) = [1 \times 10^{-4}, 1 \times 10^{-4}, 1 \times 10^{-4}]^T$. Note that all simulations for the tumor-immune dynamics based on any model in this thesis employ this initial condition unless otherwise stated, which is corresponding to the number of cells and the concentration of IL-2 at a level of 10^5.

Firstly, discuss the dynamics shown in the "foot-like" branch in detail. Consider the rectangular parts, in Part I ("heel area") where c ranges from 0 to $c_0 = 8.55 \times 10^{-5}$, a stable equilibrium point with large tumor population coexists with two unstable equilibrium points. As shown in Figure 2.5, the stable stationary branch collides with the upper unstable branch at bifurcation c_0. Within Part I, the population of tumor cells would either boom up monotonously or shrink slightly to the stable steady state based on the initial condition. Figure 2.7 shows the temporal dynamics of effector cells, tumor cells and IL-2 at $c = 1 \times 10^{-5}$.

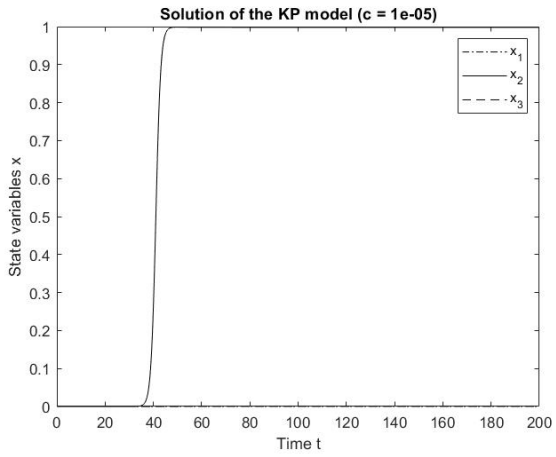

Figure 2.7 Dynamics of non-treatment KP Model at $c = 1 \times 10^{-5}$

In Part II ("instep area") where c ranges from c_0 to $c_1 = 0.0326$, a branch of unstable equilibrium points and a branch of stable periodic orbits are discovered. Figure 2.6 presents the bifurcation diagram in a semi-logarithmic coordinate system to show the unclear periodic part before c_1 in Figure 2.4. As displayed in Figure 2.8, the tumor population converge to a periodic orbit regardless of the initial conditions under the immunological surveillance. In a single period, the tumor stays at a dormant status that only few cells persist for most of the time. During the dormant status, the tumor population is probably too small to discover. However, the population of tumor bursts suddenly implying the recurrence of tumor, which is extremely common in clinics. Within Part II, the immune response behaves more intense as the antigenicity of effector cells enhances. The periodic orbit shrinks as well as the recurrence period. Table 2.2 compares the periodic tumor dynamics at $c = 0.02$ and $c = 0.03$ with the same initial condition in terms of the maximum value, the amplitude of periodic orbits and the recurrence period. Both the maximum tumor population in general and in period status decline as c increases, and the recurrence period shortens.

c	Non-dimensional tumor dynamics			Dimensional tumor dynamics		
	Maximum value	Periodic amplitude	Period	Maximum value	Periodic amplitude	Period
0.02	3.7×10^{-4}	3.7×10^{-4}	43.6	3.7×10^{5} cells	3.7×10^{5} cells	242days
0.03	1.3×10^{-4}	6.9×10^{-5}	19.3	1.3×10^{5} cells	6.9×10^{4} cells	107days

Table 2.2 Comparison of the periodic tumor dynamics at $c = 0.02$ and $c = 0.03$

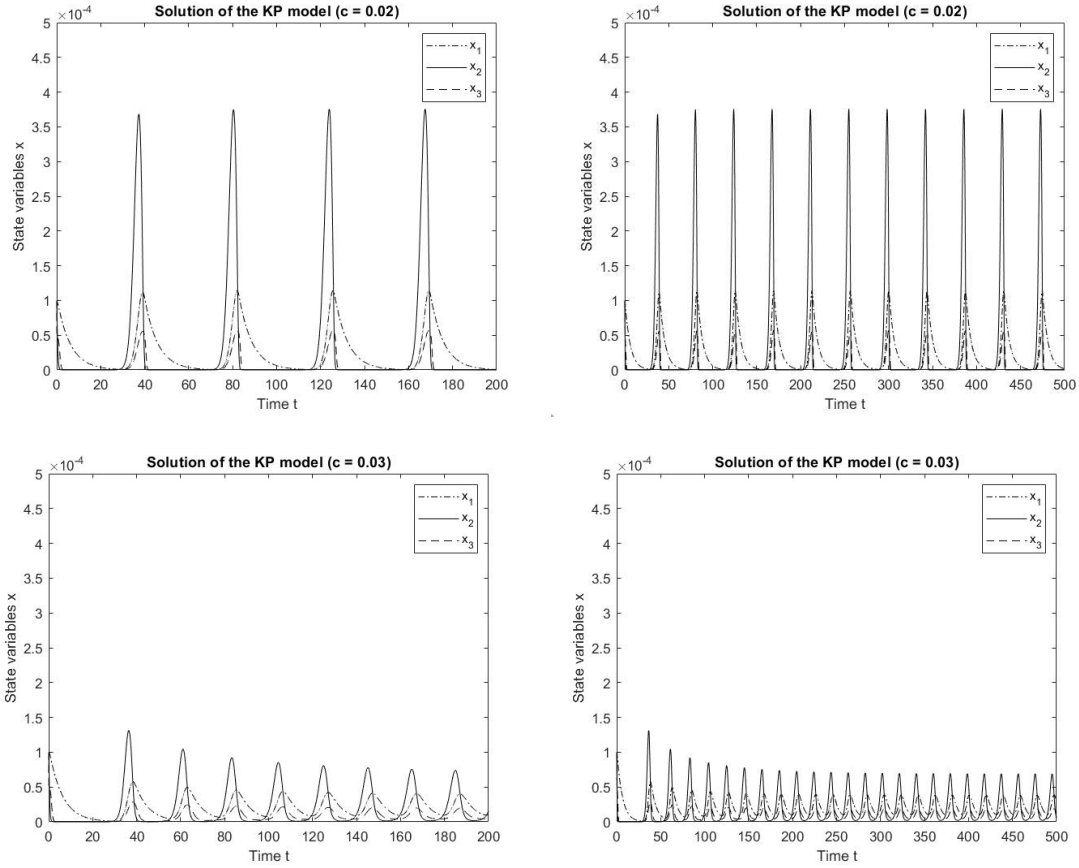

Figure 2.8 Dynamics of non-treatment KP Model at $c = 0.02$ and $c = 0.03$

In Part III ("toe area"), Hopf bifurcation occurs at c_1, where the stable branch of limit cycles bifurcates from the stable equilibrium branch. There is a unique stable focus with rather small value in Part III. This area refers to a "safe" tumor status that the tumor population keeps small and harmless to the host. Figure 2.9 shows that the tumor

population converges oscillatorily to a stable status. Table 2.3 compares the tumor dynamics with $c = 0.035$ and $c = 0.04$, in terms of the second peak value, the steady state and the converge time. The tumor population converges faster and reaches a lower stable amount with a higher value of c.

c	Non-dimensional value			Dimensional value		
	2nd peak value	Steady state	Converge time	2nd peak value	Steady state	Converge time
0.035	9.8×10^{-5}	1.8×10^{-5}	~700	9.8×10^{4}	1.8×10^{4}	~10.7years
0.04	7.8×10^{-5}	1.6×10^{-5}	~300	7.8×10^{4}	1.6×10^{4}	~4.6years

Table 2.3 Comparison of the periodic tumor dynamics at $c = 0.035$ and $c = 0.04$

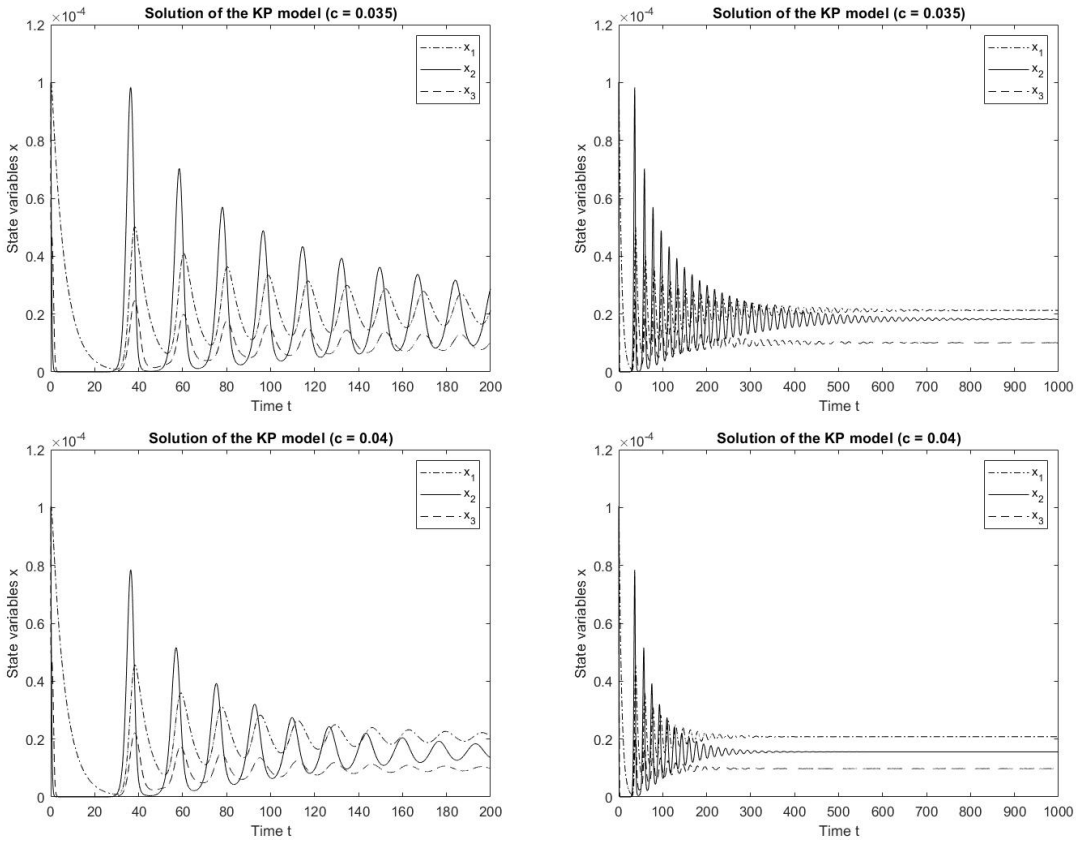

Figure 2.9 Dynamics of non-treatment KP Model at $c = 0.035$ and $c = 0.04$

CHAPTER THREE CONTROL OF IMMUNOTHERAPIES

This chapter applies and analyzes several control strategies on the immunotherapies based on the KP model in order to eradicate tumors or inhibit tumor growths. Specifically, an open-loop control constructs an ideal stable equilibrium point at tumor-free state. This local tumor-free equilibrium point indicates that regular quantitative immunotherapy could cure the tumor whose initial condition is not far from the stable equilibrium point. While the stability of this local tumor-free equilibrium point is independent of c, it is observed that the range of the stability depends on the antigenicity. Furthermore, this research also attempts to modify the tumor-immune interactions via bifurcation control with washout filters based on the bifurcation structure of the system itself. The bifurcation control aims to extend the "safe" equilibrium branch area and reduce the amplitude of the periodic orbits discovered by the KP model and discussed in the last chapter.

3.1 Open-Loop Control and Dynamic Analysis

This section studies the dynamics of the tumor-immune response with open-loop control. Constant control input u_1 and u_2 implies regular quantitative implantation of ACI and IL-2, respectively. This open-loop control aims to construct an asymptotically stable equilibrium point at the tumor-free state, i.e., an equilibrium point

$$\boldsymbol{x_{ss}} = (x_1{}^*, 0, x_3{}^*) \tag{3.1}$$

with positive constant $x_1{}^*$ and $x_3{}^*$. The equilibrium point at the origin of the KP model without treatment, i.e., the all-zero state independent of c, naturally generates the open-loop control idea. All-zero state implicates that there are no effector cells, IL-2 and

tumor cells in a living host. This status is neither possible nor desired. Although the unstable all-zero equilibrium point makes no sense in an immune system, it raises the question if it is possible to construct a stable equilibrium point with a zero x_2 state, representing the tumor-free status with bounded effector cells and IL-2. The simplest solution for constructing such an equilibrium point is by applying constant feedforward control.This part first revises Kirschner and Panetta's work [15] on the condition of applying ACI and IL-2 that can eliminate tumors in the open-loop control system. The thesis analyzed the open-loop system from the perspective of control designing, while they focus on comparing the treatment effects of various immunotherapies and guiding their dosage. Furthermore, the thesis applies a specific treatment combining ACI and IL-2, which raises the problem of estimating the region of attraction of the tumor-free state. Several attempts have been conducted on the estimation.

Based on the most general KP model, equation (2.4)-(2.5), add constants feedforward control inputs s_1 and s_2 into the first and third equations respectively in order to move the equilibrium point from origin to the desired tumor-free status. The state model of the open-loop control system

$$\dot{\boldsymbol{x}} = \boldsymbol{f_o}(\boldsymbol{x}) \tag{3.2}$$

turns to be

$$\frac{dx_1}{dt} = cx_2 - \mu_2 x_1 + \frac{p_1 x_1 x_3}{g_1 + x_3} + s_1 \tag{3.3}$$

$$\frac{dx_2}{dt} = r_2 x_2(1 - bx_2) - \frac{ax_1 x_2}{g_2 + x_2} \tag{3.4}$$

$$\frac{dx_3}{dt} = \frac{p_2 x_1 x_2}{g_3 + x_2} - \mu_3 x_3 + s_2, \tag{3.5}$$

where s_1 and s_2 are positive scalars. Solve the new equilibrium point via

$$\dot{\boldsymbol{x}}_{\boldsymbol{ss}} = \boldsymbol{f}_{\boldsymbol{o}}(\boldsymbol{x}_{\boldsymbol{ss}}) = \mathbf{0}. \tag{3.6}$$

The desired tumor-free equilibrium point in terms of s_1 and s_2 is

$$\boldsymbol{x}_{\boldsymbol{ss}} = ({x_1}^*, 0, {x_3}^*) = \left(\frac{\mu_3 g_1 s_1 + s_1 s_2}{\mu_2 \mu_3 g_1 + (\mu_2 - p_1) s_2}, 0, \frac{s_2}{\mu_3}\right). \tag{3.7}$$

Judge the stability of $\boldsymbol{x}_{\boldsymbol{ss}}$ by linearization. The Jacobian matrix

$$J_o = \left.\frac{\partial \boldsymbol{f}_{\boldsymbol{o}}(\boldsymbol{x})}{\partial \boldsymbol{x}}\right|_{(\boldsymbol{x}=\boldsymbol{x}_{\boldsymbol{ss}})} \tag{3.8}$$

becomes

$$\begin{bmatrix} -\mu_2 + \dfrac{p_1 {x_3}^*}{g_1 + {x_3}^*} & c & \dfrac{p_1 g_1 {x_1}^*}{(g_1 + {x_3}^*)^2} \\ 0 & r_2 - \dfrac{a {x_1}^*}{g_2} & 0 \\ 0 & \dfrac{p_2 {x_1}^*}{g_3} & -\mu_3 \end{bmatrix}. \tag{3.9}$$

The eigenvalues of the system are

$$-\mu_2 + \frac{p_1 {x_3}^*}{g_1 + {x_3}^*}, \qquad r_2 - \frac{a {x_1}^*}{g_2}, \qquad -\mu_3. \tag{3.10}$$

The equilibrium point of the nonlinear system is locally asymptotically stable if all the eigenvalues of its Jacobian matrix are positive. Then, the equilibrium point $\boldsymbol{x}_{\boldsymbol{ss}}$ is locally asymptotically stable if s_1 and s_2 satisfy that

$$s_2 < \frac{\mu_2 \mu_3 g_1}{p_1 - \mu_2} \triangleq s_{upper}^2, \qquad s_1 > \frac{g_2 r_2}{a}\left[\frac{g_2(\mu_2 - p_1) + \mu_2 \mu_3 g_1}{\mu_3 g_1 + s_2}\right] \triangleq s_{lower}^1. \tag{3.11}$$

s^2_{upper} and s^1_{lower} are defined as the upper bound of s_2 and the lower bound of s_1 respectively. s^2_{upper} is a constant while s^1_{lower} is a function of s_2. Now consider the range of s_1 and s_2 before scaling, in which case all parameters employed are unscaled. Figure 3.1 shows the function of $s^1_{lower}(s_2)$ with s_2 below $s^2_{upper} = 6.349 \times 10^7$. The area I refers to the range of s_1 and s_2 that $\boldsymbol{x_{ss}}$ is asymptotically stable in local.

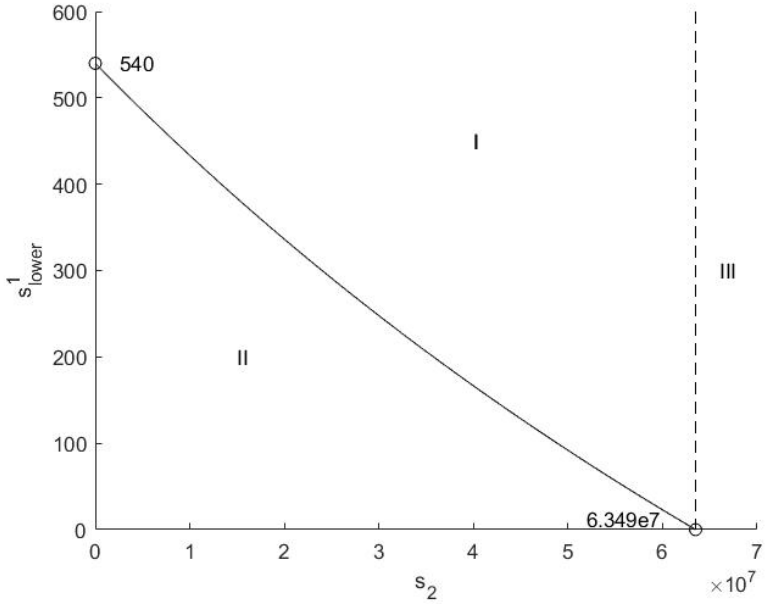

Figure 3.1 $s_2 - s^1_{lower}$ curve

Since both s_1 and s_2 are external resources, a combination of s_1 and s_2 of lower amount might be better for both the feasibility and safety of immunotherapy. As a result, the following research studies the dynamics of $s_1 = s_2 = 1 \times 10^3$.

This specific open-loop treatment results in a locally asymptotically stable equilibrium point at $\boldsymbol{x^0_{ss}} = (3.334 \times 10^4, 0, 100)$ or $\bar{\boldsymbol{x}}^{\boldsymbol{0}}_{\boldsymbol{ss}} = (3.334 \times 10^{-5}, 0{,}1 \times 10^{-7})$ independent of c. As shown in Figure 3.2, the population of tumor cells damps rapidly with the initial condition $\bar{\boldsymbol{x}}(0) = [1 \times 10^{-4}, 1 \times 10^{-4}, 1 \times 10^{-4}]^T$ c. However, the

region of attraction (ROA) of the locally asymptotically stable equilibrium point varies with c. As shown in Figure 3.3, the point $\bar{\boldsymbol{x}} = [1 \times 10^{-4}, 5 \times 10^{-4}, 1 \times 10^{-4}]^T$ is outside the ROA when $c = 1 \times 10^{-5}$ and inside the ROA when $c = 0.02$.

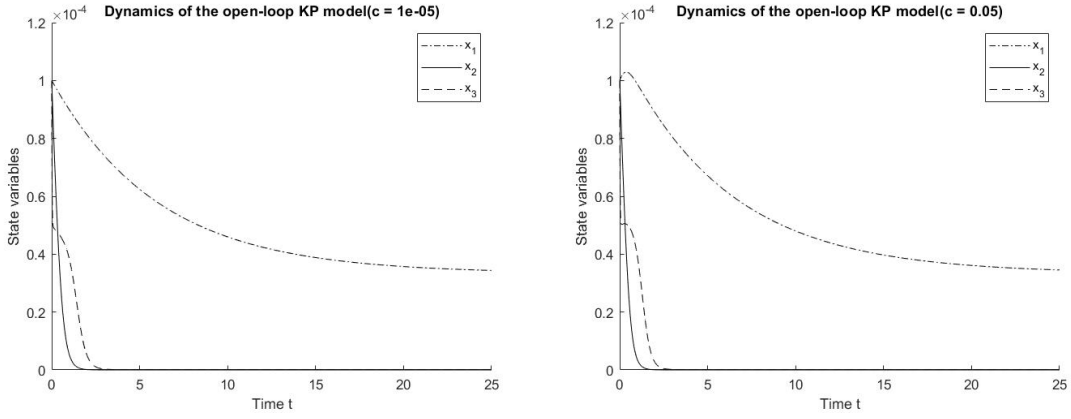

(a) $\boldsymbol{c = 1 \times 10^{-5}}$ **(b)** $\boldsymbol{c = 0.05}$

Figure 3.2 dynamics of the open-loop KP model with $\bar{x}_{20} = 1 \times 10^{-4}$

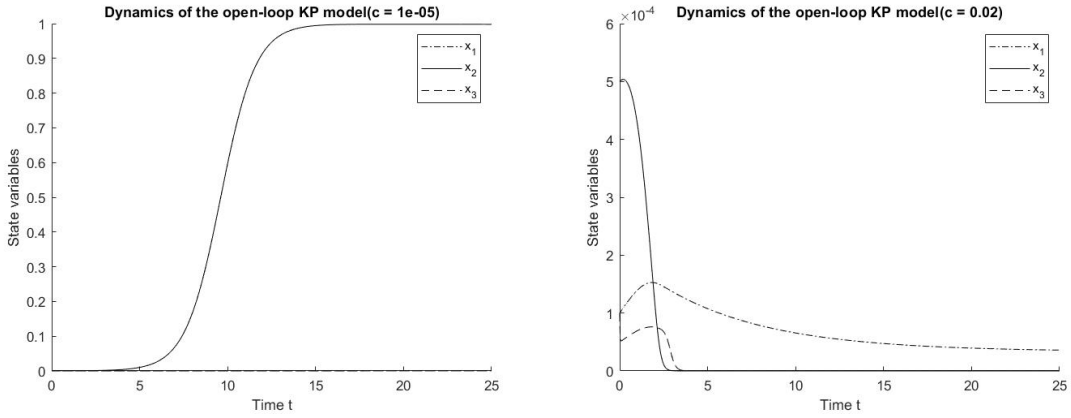

(a) $\boldsymbol{c = 1 \times 10^{-5}}$ **(b)** $\boldsymbol{c = 0.02}$

Figure 3.3 dynamics of the open-loop KP model with $\bar{x}_{20} = 5 \times 10^{-4}$

In this thesis research, simulation results of various initial conditions and parameter c show that the ROA set expands as c increases although the exact boundary of the ROA is still not clear. The ROA of the tumor-free equilibrium point refers to a three

dimensional open, connected, invariant set according to the Lemma 8.1 in [13]. The ROA set is bounded by trajectories of the system. As a result, simulations of the dynamics with multiple initial states and antigenicity values could give the exact boundary of ROA in theory. Lyapunov analysis is another option to approach a conservative ROA, but an appropriate Lyapunov function is necessary.

In summary, the open-loop control represents the regular quantitative injection of both ACI and IL-2. Within the stabilizable set of s_1 and s_2, this treatment constructs a tumor-free steady state which is locally asymptotically stable. While the value of the steady state is independent of the antigenicity, simulation results show that its region of attraction depends on the antigenicity. This ROA is a three dimensional open, connected and invariant set. In general, it is observed that the ROA extends as the antigenicity enhances. The exact ROA is not clear now. The work of finding the quantitative relationship between the antigenicity and the ROA has been left to the future.

3.2 Bifurcation Control with Washout Filters

This section applies bifurcation and amplitude control strategies on the tumor-immune system. These control approaches modify the bifurcation structures in the system to achieve desired results. Different than linear systems, the dynamics of nonlinear systems is rich and complex, often exhibiting nonlinear phenomena such as bifurcations and chaos. Bifurcation control with washout filter could adjust the behavior of a system by taking advantages of the original structure rather than destroy it. In this case, the bifurcation diagram gives the specific “foot-like” non-local structure of the nominal system along parameter c, based on the bifurcation analysis. The “toes” part, Part III with

c larger than c_1 (the Hopf bifurcation point), represents a benign condition of the tumor-immune system. It is beneficial if any treatment could enlarge this field. In the middle part of the bifurcation diagram, the amplitude of the periodic orbits increases sharply as c decrease. It is also beneficial if any treatment could reduce the amplitude of the periodic orbits.

3.2.1 Preliminaries of Bifurcation Control

Bifurcation Control with Washout Filter is dynamic feedback control. Washout filter is a stable high pass filter with a property of equilibrium preservation. Washout filter rejects steady-state input signals when transient inputs pass through the system. As a result, control with washout filters would not impact the open-loop equilibriums of the original system.

Washout filters are widely used in aircraft control systems [37] and power control systems [38]. The transfer function of washout filter takes the form

$$G(s) = \frac{y(s)}{x(s)} = \frac{s}{s+d} = 1 - \frac{d}{s+d}. \tag{3.12}$$

Here d is a positive constant, which corresponds to utilizing stable washout filters. Consider a n-dimensional state model $\dot{\boldsymbol{x}} = \boldsymbol{f}(\boldsymbol{x})$ ($x \in \mathbb{R}^n$) with steady state $\boldsymbol{x_{ss}}$. For each state x_i, introduce a washout filter state z_i, and let its transfer function to be

$$z_i(s) = \frac{1}{s+d} x_i(s). \tag{3.13}$$

The dynamic equation of the washout filter is in forms of

$$\dot{z}_i = x_i - dz_i \tag{3.14}$$

with the output equation

$$y_i = x_i - dz_i. \tag{3.15}$$

The steady state of $\boldsymbol{z}$ is $\boldsymbol{z_{ss}} = \frac{\boldsymbol{x_{ss}}}{d}$, and the output of the washout filter $y = 0$ at the steady state. It is simple to see that the equilibrium of systems would not change when applying a control input in the form

$$u = h(y) \tag{3.16}$$

such that

$$h(0) = 0. \tag{3.17}$$

Wang and Abed [27] incorporate washout filters into bifurcation and chaos control. The previous analysis explains the principle why a dynamic feedback control with washout filters would not change the equilibrium structure of a system from the perspective of exact state models. Furthermore, the property to preserve equilibriums of washout filters exists regardless of any model uncertainty that does not violate the finite dimensionality of the system. This capability under model uncertainty is beneficial greatly to the biological system since there exist large ranges of nonlinear model uncertainties due to individual differences among livings.

This thesis aims to move the Hopf bifurcation point c_1 in the KP model. Considers the system (2.2), there are pairs of purely imaginary eigenvalues when Hopf bifurcations take place. At the critical points, the linearization method (eigenvalues of the Jacobian matrix) does not work for judging the stability. Periodic limit cycles p_ϵ are bifurcated from Hopf bifurcations when c is perturbed by ϵ, the asymptotical stability of p_ϵ is determined by the characteristic exponent $\beta(\epsilon)$, which is defined by a real, smooth, even function that

$$\beta(\epsilon) = \beta_2\epsilon^2 + \beta_4\epsilon^4 + \cdots. \tag{3.18}$$

p_ϵ is orbitally asymptotically stable if $\beta(\epsilon) < 0$ and is unstable if $\beta(\epsilon) > 0$. Typically, the sign of the characteristic exponent $\beta(\epsilon)$ depends on the sign of β_2, which is called the *bifurcation stability coefficient* [39][36]. It is known that only the linear, quadratic and cubic terms possess the potential to influence the value of β_2 for a system undergoing Hopf bifurcations (or Andronov-Hopf bifurcations) [39][40][41][42]. Let the bifurcation control u consists of linear, quadratic and cubic terms in the form of

$$u = k_l y + y^T Q_u y + C_u(y, y, y), \tag{3.19}$$

where y is the vector of washout filter outputs $y_i = x_i - d_i z_i$, k_l is a real scalar, Q_u is a real symmetric $n \times n$ matrix, and C_u is a cubic form generated by a scalar-valued symmetric trilinear form. In the following control application, each term of the bifurcation with washout filter are employed and analyzed separately.

3.2.2 The Bifurcation Control Model with Washout Filters in Tumor-Immune Interactions

Consider the KP model, introduce dynamic feedback control with washout filters into the dynamics of ACI and IL-2. Give the closed-loop tumor-immune system with washout filters in a general form

$$[\dot{\boldsymbol{x}}, \dot{\boldsymbol{z}}]^T = \boldsymbol{f}(\boldsymbol{x}, \boldsymbol{z}, \boldsymbol{u}), \tag{3.20}$$

where $\boldsymbol{z} = [z_1, z_3]$ is the washout filter state. Here is the state equations of the closed-loop tumor-immune control system

$$\frac{dx_1}{dt} = cx_2 - \mu_2 x_1 + \frac{p_1 x_1 x_3}{g_1 + x_3} + u_1 \tag{3.21}$$

$$\frac{dx_2}{dt} = r_2 x_2(1 - bx_2) - \frac{ax_1 x_2}{g_2 + x_2} \tag{3.22}$$

$$\frac{dx_3}{dt} = \frac{p_2 x_1 x_2}{g_3 + x_2} - \mu_3 x_3 + u_2 \tag{3.23}$$

$$\frac{dz_1}{dt} = x_1 - d_1 z_1 \tag{3.24}$$

$$\frac{dz_3}{dt} = x_3 - d_3 z_3 \tag{3.25}$$

along with the output equations

$$y_1 = x_1 - d_1 z_1 \tag{3.26}$$

$$y_2 = x_3 - d_3 z_3 \tag{3.27}$$

$$y_3 = x_2 \tag{3.28}$$

where the control inputs are governed by real smooth functions

$$u_1 = h_1(y_1) \tag{3.29}$$

$$u_2 = h_2(y_2). \tag{3.30}$$

Note that, all the washout filter coefficients d_i are uniformly set as 0.5 without losing any generality.

3.2.3 Bifurcation Control with Linear Dynamic Feedback

In this part, we consider the linear dynamic feedback control strategy

$$u_i = -k_{li} y_i,$$

where k_{li}, so-called linear feedback gain, is a designed scalar. The objective of the linear dynamic feedback control is to either extend the region of single "safe" steady state captured by the bifurcation diagram of the non-treatment system or shrink the amplitude

of tumor recurrences, via moving the Hopf bifurcation that marks the lower boundary of the "toe area" to a smaller c. The influence of this closed-loop treatment is analyzed in AUTO.

1) Adoptive cellular immunotherapy ($u_1 = -k_{l1}y_1, u_2 = 0$)

Consider the situation that only adoptive cellular immunotherapy is applied. k_{l1} is the constant (linear) feedback gain of the washout filter. $k_{l1} < 0$ refers to implanting activated anti-tumor effector cells into the patient, while $k_{l1} > 0$ indicates an initiative action to reduce the amount of the effector cells. Despite that, to the best of the author's knowledge, there is no immunotherapy treatment aiming to reduce the amount of the effector cells, this research could still provide an idea to structurally improve a system with complex nonlinear phenomena under modeling uncertainty.

Routh criterion is commonly used to theoretically analyze the controllable set of k_l, however, hardly could it be employed here due to the mathematically intricate model. Therefore, this research numerically calculates, via AUTO, the Hopf bifurcation of the closed-loop control systems with varying values of the feedback gain, in order to find the controllable range. According to the previous study, the bifurcation point of the non-treatment tumor-immune system is at $c_1 = 3.26 \times 10^{-2}$, and the physically valid range of the antigenicity c is [0, 0.05]. Figure 3.4 (a) shows the range of k_{l1} moving the bifurcation points in both directions, that either c_1 increases or decreases, within the physically valid range of c. c_1 moves to left (decrease) under the control of $k_{l1} \in (0, 0.034]$, and moves to right (increase) under the control of $k_{l1} \in [-0.19, 0) \cup (0.034, 1.3)$. Figure 3.4 (b) shows the part that c_1 moves to the left, under which the

"safe equilibrium" area extends. This curve shows that the minimum value of c_1 takes place within (0.11, 0.16) at $c_1 = 3.09 \times 10^{-2}$.

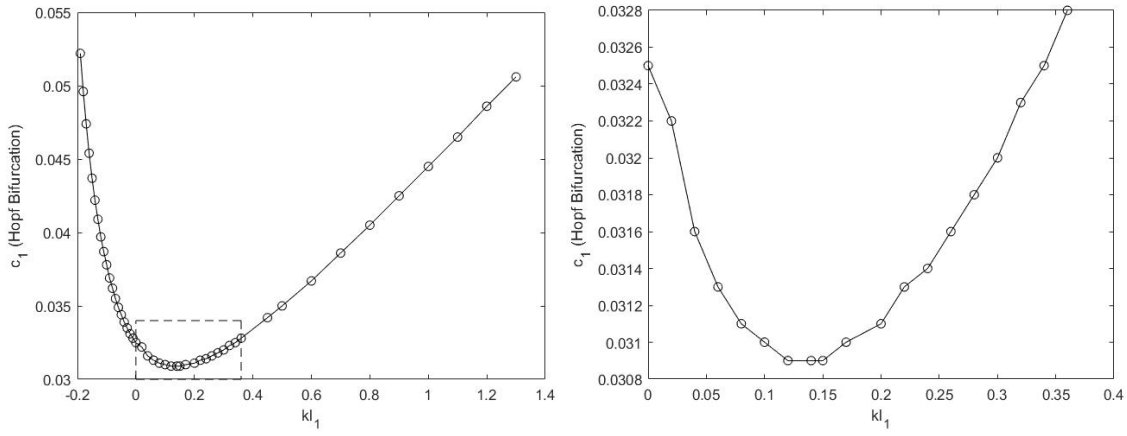

(a) **(b)**

Figure 3.4 $k_{l1} - c_1$ curve

The above discussion shows the capability of the linear, dynamic feedback control along the state x_1 to place the Hopf bifurcation point of the tumor-immune system to any point inside $c_1 \in [3.09, 0.05] \times 10^{-2}$. Figure 3.5 (a) and (b) shows the bifurcation diagram, along parameter c, at $k_{l1} = 0.013$ and $k_{l1} = -0.018$ representing the limit movability to left and right, respectively. Compared to Figure 2.6, the bifurcation diagram of the non-treatment KP model, Auto shows that the left-side movability of Hopf bifurcation is limited, while the right-side movability is strong via linear dynamic feedback control with washout filters.

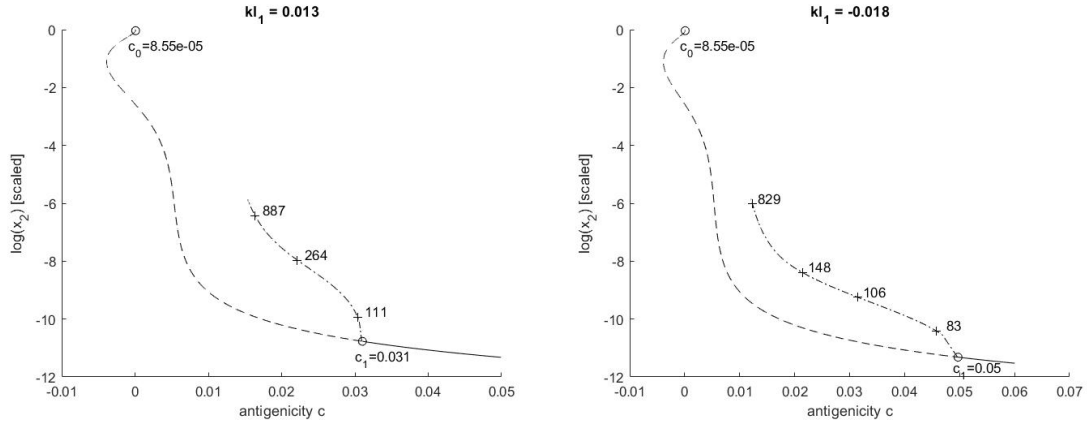

(a) $k_{l1} = 0.013$ **(ultimate movability to left)(b)** $k_{l1} = -0.018$ **(ultimate movability to right)**

Figure 3.5 the bifurcation diagrams of the closed-loop tumor-immune system with linear dynamic control along x_1

Besides the movability of Hopf bifurcation, it is shown that the linear dynamic feedback control also changes the amplitude and the periods of limit cycles in the "instep area". Consider the KP model with two representative fixed values of the antigenicity, $c = 0.02$, and $c = 0.04$, presenting Part II (periodic orbits) and Prat III (safe equilibrium) of the bifurcation structure of the non-treatment KP model respectively. Figure 3.6 (a) and (b) shows the influence of the constant control gain k_{l1} to the tumor dynamics. These figures compare the tumor involution under the linear dynamic washout control among the non-treatment case and two limit-movability cases for the Hopf bifurcation.

According to the tumor involution, while the range of "safe" single equilibrium extends, the amplitude of periodic orbits amplifies at the same time. The increase of the amplitude is limited with a limited left-side movability of the linear dynamic feedback control. In the other direction, though the bifurcation control with $k_l = -0.18$ shrinks the region of "safe equilibrium", it reduces the amplitude of the first tumor explosion and the following tumor relapses at lower antigenicity levels. At $c = 0.02$, the control with $k_l =$

-0.18 lead to an around twenty percent reduction in the peak of tumor dynamics, which is around 2×10^{-4} after scaling and 2×10^{5} cells. In the aspect of the time period, the control with $k_l = -0.18$ shortens the recurrence period by one third at $c = 0.02$.

In summary, the linear dynamic feedback control with washout filters is able to move the Hopf bifurcation slightly to left and arbitrarily to right. By implanting ACI in the designed way, the amplitude of the tumor growth significantly drops at a lower antigenicity level. However, this treatment is also at risk of shortening the recurrence periods and extending the area where periodic orbits generate.

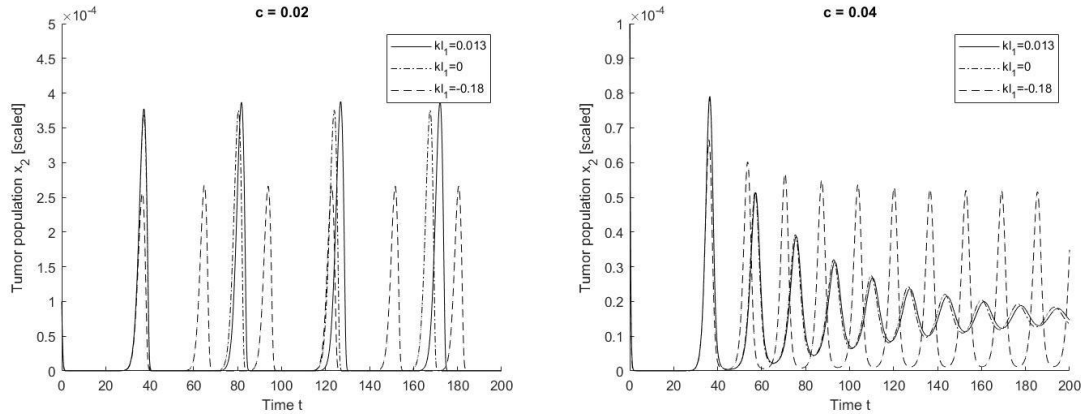

(a) $\boldsymbol{c = 0.02}$ **(b)** $\boldsymbol{c = 0.04}$

Figure 3.6 The influence of the constant control gain k_{l1} to the tumor dynamics of the closed-loop KP model with linear dynamic control along x_1

2) Interleukin-2 ($u_1 = 0, u_2 = -k_{l2}y_2$)

A simulation test of linear, dynamic feedback control strategy along x_3 (IL-2) is also applied. However, the numerical analysis of this closed-loop system with $u_3 = -k_{l3}y_3$ shows no noticeable change in either the tumor dynamics or the bifurcation diagram.

3.2.4 Amplitude Control with Quadratic or Cubic Dynamic Feedback

This thesis also studies the effect of amplitude control with quadratic and cubic dynamic feedback in ACI and IL-2. There was an expectation that the quadratic or cubic dynamic feedback with washout filters could modify the amplitude of the periodic orbits in the "instep area".

The quadratic dynamic feedback control employs

$$u_i = k_{qi} {y_i}^2 \tag{3.31}$$

and the cubic dynamic feedback control employs

$$u_i = k_{ci} {y_i}^3. \tag{3.32}$$

where constant k_{qi} and constant k_{ci} is the quadratic feedback gain and the cubic feedback gain, respectively.

Controllability theories of linear systems do not apply for the linearized nonlinear system with dynamic feedback control. The simulation and AUTO results show that there is no noticeable change of tumor dynamics with either quadratic or cubic dynamic feedback control with washout filters along x_1 and x_3.

Though the effect of quadratic and cubic dynamic control with washout filters are limited in the KP model, it is possible to employ them into other tumor-immune system or tumor therapy models that undergo Hopf bifurcations.

CHAPTER FOUR CONCLUSIONS AND FUTURE WORK

3.1 Conclusions

This thesis reviews the KP model in bifurcation analysis and part of the open-loop treatments with immunotherapies of ACI and IL-2. Based on Kirschner's works [15] on the open-loop control analysis, this thesis also makes an attempt to analyze the region of attraction of the open-loop control. Based on the understanding of the tumor-immune mechanism explained by the KP model, bifurcation control with washout filters is applied to promote the effects of immunotherapies. Different from the open-loop treatment, the dynamic feedback with washout filters remains the equilibrium branches of the original system. This feature is beneficial to systems under uncertainties, which is a common situation in biological models due to individual differences. In the future, the bifurcation control with washout filter could be extended into other models of tumor therapies undergoing Hopf bifurcations or chaos.

The classic KP model explains the non-local dynamics of tumor-immune interactions involves the effector cells, tumor cells, and IL-2. Two bifurcation branches represent the evolution of the tumor population along with the antigenicity. One is a single unstable equilibrium point at the origin, which is independent of c. Within another branch, the dynamics of tumor growth changes qualitatively along parameter c, the antigenicity of effector cells. The system possesses a "dangerous" equilibrium close to its carrying capacity with a tiny c. As c increases, periodic orbits generate representing the neoplasm recurrence. Finally, as c passes through the Hopf bifurcation, a "safe" equilibrium point appears.

It is shown that regular quantitative treatment combing the ACI and IL-2 constructs a new tumor-free equilibrium point independent of c. This tumor-free equilibrium is locally asymptotically stable. The simulation results show that the region of attraction of the tumor-free equilibrium tends to increase as c increases.

It is known that only linear, quadratic and cubic terms are potentially to change the stability of a nonlinear system undergoing Hopf bifurcations indirectly via β_2. As a result, this thesis applies the linear, quadratic, cubic dynamic feedback control with washout filters separately into the KP model. It is shown that a linear dynamic feedback treatment with washout filter in ACI is likely to suppress the tumor growth by moving the Hopf bifurcation. Qualitatively implanting activated anti-tumor cells flowing the linear dynamic control could shrink the amplitude of the tumor recurrences but shorten the time periods simultaneously. Simulations and AUTO results indicate that a linear dynamic feedback treatment with washout filter in IL-2 presents no noticeable effect, as well as a quadratic and cubic dynamic feedback treatments with washout filter in both ACI and IL-2.

This thesis attempts to guide the immunotherapies combining ACI and IL-2. The behavior of a tumor-immune system highly depends on the antigenicity. A combination treatment of ACI and IL-2 have the potentiality to eradicate tumors, but the region of attraction turns to reduce as the effector cells become less sensitive to tumor cells. When the initial condition is out of the region of attraction, tumor booms up, and this situation could be lethal to patients. To avoid this tragedy, implanting the activated anti-tumor cells under a bifurcation control with ACI first might be an option when the antigenicity

of patients is at a low level. The open-loop treatment could be applied later after that the dynamics of the tumor-immune interactions has dropped into the range of action.

Furthermore, biological systems have individual differences, and it is challenging to apply precise measurements in a living system. The bifurcation control with washout filters has strength in mitigating the potential negative impact from the modeling uncertainties.

3.2 Future Work

Further work is needed in the control treatment based on the KP model. Several works have been tried to better estimate the region of attraction of the tumor-free equilibrium point in the open-loop KP system in section 3.1. Though the results are limited, one direction is to find an appropriate Lyapunov function to estimate ROA. It is meaningful if the quantitative relationship between the ROA and the antigenicity c becomes clear.

Bifurcation control, either with or without washout filters, can be good options for control applications in tumor treatments and other biological systems. The controlled response benefits from remaining the equilibrium structure regardless of model uncertainties. This thesis research has also considered and studied a tumor-immune-virus system [43] where an equilibrium branch bifurcates to chaos. Control of nonlinear phenomena such as bifurcations and chaos in biological systems can be a fruitful research area.

BIBLIOGRAPHY

[1] H. Enderling, M.A. Chaplain. Mathematical modeling of tumor growth and treatment. Current Pharmaceutical Design, 20(30): 4934–4940, 2014.

[2] B. D. Curti, A. C. Ochoa, W. J. Urba, W. G. Alvord, W. C. Kopp, G. Powers, C. Hawk, S. P. Creekmore, B. L. Gause, J. E. Janik, J. T. Holmlund, P. Kremers, R. G. Fenton, L. Miller, M. Sznol, J. W. Smith II, W. H. Sharfman and D. L. Longo. Influence of interleukin-2 regimens on circulating populations of lymphocytes after adoptive transfer of anti-CD3-stimulated T cells: Results from a phase I trial in cancer patients. Journal of Immunotherapy, 19(4): 296-308, 1996.

[3] B. L. Gause, M. Sznol, W. C. Kopp, J. E. Janik, J. W. Smith II, R. G. Steis, W. J. Urba, W. Sharfman, R. G. Fenton, S. P. Creekmore, J. Holmlund, K. C. Conlon, L. A. VanderMolen and D. L. Longo. Phase I study of subcutaneously administered interleuking- 2 in combination with interferon alfa-2a in patients with advanced cancer. Journal of Clinical Oncology, 14(8): 2234-2241, August 1996.

[4] I. Hara, H. Hotta, N. Sato, H. Eto, S. Arakawa and S. Kamidono. Rejection of mouse renal cell carcinoma elicited by local secretion of interleukin-2. Japanese Journal of Cancer Research, 87: 724-729, 1996.

[5] R. Kaempfer, L. Gerez, H. Farbstein, L. Madar, O. Hirschman, R. Nussinovich and A. Shapiro. Prediction of response to treatment in superficial bladder carcinoma through pattern of interleukin-2 gene expression. Journal of Clinical Oncology, 14(6): 1778-1786, June 1996.

[6] U. Keilholz, C. Scheibenbogen, E. Stoelben, H. D. Saeger and W. Hunstein. Immunotherapy of metastatic melanoma with interferon-alpha and interleukin-2: Pattern of progression in responders and patients with stable disease with or without resection of residual lesions. European Journal of Cancer, 30A(7): 955-958, 1994.

[7] Angela J. Lumsden, James P. Codde, Peter H. Van Der Meide and Bruce N. Gray. Immunohistochemical characterisation of immunological changes at the tumour site after chemo-immunotherapy with doxorubicin, interleukin-2 and interferon-c. Anticancer Research, 16: 1145Ð1154, 1996.

[8] F. M. Marincola, D. E. White, A. P. Wise and S. A. Rosenberg. Combination therapy with interferon alfa-2a and interleukin-2 for the treatment of metastatic cancer. Journal of Clinical Oncology, 13(5): 1110-1122, 1996.

[9] H. Rabinowich, M. Banks, T. E. Reichert, T. F. Logan, J. M. Kirkwood and T. L. Whiteside. Expression and activity of signaling molecules n T lymphocytes obtained from patients with metastatic melanoma before and after interleukin 2 therapy. Clinical Cancer Research, 2: 1263-1274, 1996.

[10] S. A. Rosenberg, J. C. Yang, S. L. Topalian, D. J. Schwartzentruber, J. S. Weber, D. R. Parkinson, C. A. Seipp, J. H. Einhorn and D. E. White. Treatment of 283 consecutive patients with metastatic melanoma or renal cell cancer using high-dose bolus interleukin 2. JAMA: The Journal of the American Medical Association, 271(12): 907-913, 1994.

[11] M. Rosenstein, S. E. Ettinghousen and S. A. Rosenberg. Extravasion of intravascular fluid mediated by the systemic administration of recombinant interleukin 2. Journal of Immunology, 137(5): 1735-1742, Sep 1986.

[12] D. J. Schwartzentruber. In Vitro predictors of clinical response in patients receiving interleukin-2-based immunotherapy. Current Opinion in Oncology, 5: 1055-1058, 1993.

[13] H. K. Khalil. Nonlinear systems. Englewood Cliffs, NJ: Prentice-Hall, 1996.

[14] V. A. Kuznetsov, I. A. Makalkin, M. A. Taylor and A. S. Perelson. Nonlinear dynamics of immunogenic tumors: Parameter estimation and global bifurcation analysis. Bulletin of Mathematical Biology, 56(2): 295-321, 1994.

[15] D. Kirschner and J. C. Panetta. Modeling immunotherapy of the tumor-immune interaction. Journal of Mathematical Biology, 37: 235-252, 1998.

[16] C. DeLisi and A. Rescigno. Immune surveillance and neoplasia - I: a minimal mathematical model. Bulletin of Mathematical Biology, 39: 201-221, 1977.

[17] J. A. Adam. Effects of vascularization on lymphocyte/tumor cell dynamics: Qualitative features. Mathematical and Computer Modelling, 23(6): 1-10, 1996.

[18] F. K. Nani and M. N. Oğuztöreli. Modelling and simulation of Rosenberg-type adoptive cellular immunotherapy. IMA Journal of Mathematics Applied in Medicine & Biology, 11: 107-147, 1994.

[19] R. J. DeBoer, Pauline Hogeweg, Hub F. J. Dullens, Roel A. DeWeger and Willem DenOtter. Macrophage T Lymphocyte interactions in the anti-tumor immune response: A mathematical model. The Journal of Immunology, 134(4): 2748-2758, April 1985.

[20] N. Bellomo, L. Preziosi. Modelling and mathematical problems related to tumor evolution and its interaction with the immune system. Mathematical and Computer Modelling, 32 (34): 413-452, 2000.

[21] L.G. de Pillis, Gu W., A. Radunskaya. Mixed immunotherapy and chemotherapy of tumors: Modeling, applications and biological interpretations. Journal of Theoretical Biology, 238 (4): 841-862, 2006.

[22] F. A. Rihan, S. Lakshmanan, H. Maurer. Optimal control of tumour-immune model with time-delay and immuno-chemotherapy. Applied Mathematics and Computation, 353: 147-165, 2019.

[23] D.G. Mallet, L.G. De Pillis. A cellular automata model of tumor–immune system interactions. Journal of Theoretical Biology, 239 (3): 334-350, 2006.

[24] T.L. Chien, C.C. Chen, C.J. Huang. Feedback linearization control and its application to MIMO cancer immunotherapy. IEEE Transactions on Control Systems Technology, 18(4): 953-961, 2010.

[25] S. A. Rosenberg, M. T. Lotze. Cancer immunotherapy using interleukin-2 and interleukin-2-activated lymphocytes. Annual Review of Immunology, 4: 681-709, 1986.

[26] E. H. Abed, H. O. Wang, and A. Tesi. Control of bifurcations and chaos. In W. S. Levine, editor, The Control Handbook, 951-966. CRC Press & IEEE Press, Boca Raton, FL, 1995.

[27] H. O. Wang, E. H. Abed. Bifurcation control of a chaotic system. Automatica, 31 (9): 1213-1226, 1995.

[28] McAneney H, O'Rourke SFC. Investigation of various growth mechanisms of solid tumour growth within the linear-quadratic model for radiotherapy. Physics in Medicine and Biology, 52(4): 1039-54, 2007.

[29] Gompertz B. On the nature of the function expressive of the law of human mortality, and on a new mode of determining the value of life contingencies. Philosophical Transactions of the Royal Society of London, 115: 513-583, 1825.

[30] Winsor CP. The Gompertz curve as a growth curve. Proceedings of the National Academy of Sciences of the United States of America, 18(1): 1-8, 1932.

[31] Prehn RT. The inhibition of tumor growth by tumor mass. Cancer Research, 51(1): 2-4, 1991.

[32] E. J. Doedel. AUTO, a program for the automatic bifurcation analysis of autonomous systems. Congressus Numerantium, 30: 265-284, 1981.

[33] E. J. Doedel, R. C. Paenroth, A. R. Champneys, T. F. Fairgrieve, Y. A. Kuznetsov, B. E. Oldeman, B. Sandstede and X. J. Wang. AUTO2000: Software for continuation and bifurcation problems in ordinary differential equations. Technical report, California Institute of Technology, Pasadena CA, 2000.

[34] E. J. Doedel, A. R. Champneys, T. F. Fairgrieve, Y. A. Kuznetsov, B. E. Oldeman, R. C. Paenroth, B. Sandstede, X. J. Wang and C. H. Zhang. AUTO-07P: Continuation and bifurcation software for ordinary differential equations. Technical report, California Institute of Technology, Pasadena CA, 2007.

[35] G. Iooss and D. D. Joseph. Elementary stability and bifurcation theory. Springer, New York. 1980.

[36] D. Chen. Control and anti-control of bifurcations with applications to cardiac system and Rayleigh-Benard convection. M.S. Thesis, ECE, Duke University, 1999.

[37] B. L. Stevens and F. L. Lewis. Aircraft Control and Simulation. Wiley, New York, 1992.

[38] P. M. Anderson and A. A. Fouad. Power system Control and Stability. Iowa State University Press, Ames, IA, 1977.

[39] E. H. Abed and J. H. Fu. Local feedback stabilization and bifurcation control: Part I. Hopf bifurcation. Systems & Control Letters, 7: 11-17, 1986.

[40] J. E. Marsden and M. McCracken. The Hopf Bifurcation and Its Applications. Springer-Verlag, New York, 1976.

[41] J. H. Fu and E. H. Abed. Families of Lyapunov functions for nonlinear systems in critical cases. IEEE Transactions on Automatic Control, AC-38, 3-16, 1993.

[42] B. D. Hassard, N. D. Kazarinoff and Y. H. Wan. Theory and Applications of Hopf Bifurcation. Cambridge University Press, 1981.

[43] R. Eftimie, C. MacNamara, J. Dushoff, J. L. Bramson and D. J. D. Earn. Bifurcations and chaotic dynamics in a tumour-immune-virus system. The Mathematical Modelling of Natural Phenomena, 11 (5): 65–85, 2016.

CURRICULUM VITAE